

## General Disclaimer

### One or more of the Following Statements may affect this Document

- This document has been reproduced from the best copy furnished by the organizational source. It is being released in the interest of making available as much information as possible.
- This document may contain data, which exceeds the sheet parameters. It was furnished in this condition by the organizational source and is the best copy available.
- This document may contain tone-on-tone or color graphs, charts and/or pictures, which have been reproduced in black and white.
- This document is paginated as submitted by the original source.
- Portions of this document are not fully legible due to the historical nature of some of the material. However, it is the best reproduction available from the original submission.

EXPERIMENTAL DETERMINATION OF SOUND AND HIGH-SPEED FLOW INTERACTION

Edward Lumsdaine  
Mechanical and Aerospace Engineering Department, University of Tennessee  
Knoxville, Tennessee 37916, U.S.A.

Richard Silcox  
Acoustics Branch, NASA Langley Research Center  
Hampton, Virginia 23665, U.S.A.

N77-23898

Unclass  
26033

G3/71

CSCCL 20A

(NASA-TM-X-74688) EXPERIMENTAL  
DETERMINATION OF SOUND AND HIGH-SPEED FLOW  
INTERACTION (NASA) 9 P HC A02/MF A01

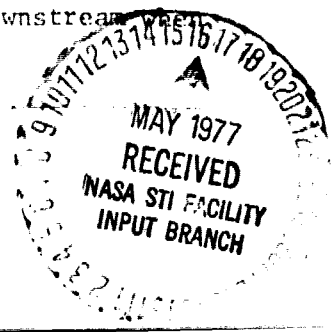
1. INTRODUCTION

The attenuation of sound at different frequencies and modes in a finite duct with high-speed flow (with or without an axial pressure gradient) is a difficult problem to solve analytically, even with numerous assumptions. Experimentally, two conditions must be met in order to obtain meaningful data. The first is the requirement of producing a sound field of different modes with sufficient intensity, the second is to provide an air stream that has minimal background noise. This paper describes a facility that was used to measure the interaction of flow with sound at high Mach numbers. Four inlets with different area variations (or axial gradients) were tested. Sound of selected frequencies and modes (0,0), (1,0), (2,0) was generated with eight circumferential acoustic drivers.

2. DESCRIPTION OF TEST FACILITY AND INLETS

The tests were conducted in the anechoic chamber transonic compressor facility of the NASA Langley Research Center. The test vehicle was a 30.5 cm tip diameter single-stage transonic compressor with 19 rotor blades. Figure 1 shows the anechoic chamber facility with one of the test inlets in place. Also shown in the figure are the choked inlet, the wall microphones, the acoustic drivers, static pressure taps, and the acoustic traverse probe.

Four inlets were tested representing four different axial velocity gradients. The first is a zero velocity gradient inlet (constant-area duct); the second has its maximum velocity gradient toward the back of the inlet; the third has a constant velocity gradient, and the fourth has its maximum velocity gradient near the throat. Figure 2 shows the area variation of these four inlets. These inlets were designed to produce minimum boundary layer separation. However, the aerodynamic data indicated that the flow in inlet number four separated near the throat and reattached downstream the throat velocity was near transonic speeds.



### 3. INSTRUMENTATION AND TEST PROCEDURE

Figure 3 is a schematic of the inlet arrangement, showing the position of the wall microphones. Figure 4 is a schematic of the test section together with the choked inlet (with centerbody), showing the position of the pressure probes for aerodynamic measurements. In addition to the eight wall microphones, nine far-field microphones were used to obtain data in the radiation field. Aerodynamic output was recorded on VIDAR from the scanivalve system with on-line chart output as well as magnetic tape. The far-field data were taken on-line with a 1/3-octave real-time analyzer.

#### Aerodynamic Instrumentation:

1. 72 static pressure taps were located axially on the test section and choked inlet (36 each) for obtaining the Mach number distribution along the walls. In addition, four static taps distributed circumferentially at two axial locations were used to determine the circumferential pressure variation.
2. One total pressure probe at the exit of the test section was used to determine the pressure loss and mass flow.
3. The centerbody of the choked inlet was controlled by a hydraulic cylinder, and its position was indicated by a voltmeter at the control panel.

#### Acoustic Instrumentation:

1. Nine 1/2-inch condenser microphones located 4.57 m ahead of the inlet plane and reading at every 10 degrees (but excluding the 90-degree position) were used to obtain far-field acoustic data.
2. Eight B&K 1/4-inch condenser microphones were located axially in the test section to determine the in-duct pressure distribution.
3. Four 1/4-inch condenser microphones located circumferentially halfway along the axis of the test section were used to monitor the waves generated by the drivers, in order to ensure that the desired modes were produced.
4. Eight acoustic drivers (ID-60, Universal Sound Units, 60 Watts, 16 Ohms) were used to generate the desired modes. The arrangement of the drivers together with the monitoring system is shown in Figure 5.

#### Test Procedure:

All microphones were calibrated before each test. Prior to starting the compressor, a no-flow test was conducted for each frequency and mode. The frequencies on the sine-random generator (B&K 1022) were selected for each case above the cut-off for that particular mode; they were:

<u>Mode (0,0)</u>	<u>Mode (1,0)</u>	<u>Mode (2,0)</u>
500 Hz	764 Hz	1223 Hz
680 Hz	1000 Hz	1490 Hz
1000 Hz	1600 Hz	2000 Hz

The output signal from the sine-random generator was fed into an eight-channel phase shifter where each channel was separately adjusted in phase and amplitude. The three modes were generated by the eight-channel phase shifter by placing the sound drivers in accordance with the following table:

Sound Driver	1	2	3	4	5	6	7	8
Mode (0,0)	0°	0°	0°	0°	0°	0°	0°	0°
Mode (1,0)	0°	45°	90°	135°	180°	225°	270°	315°
Mode (2,0)	0°	90°	180°	270°	0°	90°	180°	270°

The phase adjustments to produce any mode of order (m,0) are given by the relation

$$\theta \text{ (degrees)} = \frac{360 m(i-1)}{8}, \quad i = 1, 2, \dots, 8 \text{ (number of drivers).}$$

The output from each channel was fed into the phase meter to measure the phase angle. The output level of each sound driver was monitored by using the digital voltmeter which measured the voltage output from each channel. Typical results are given in Figure 6.

For testing of the inlets under flow conditions, the centerbody of the choked inlet was in the retracted position, and the compressor was then accelerated until choking in the inlet occurred. After data collection in this position, the centerbody was translated consecutively to several prescribed positions to give the different desired axial Mach numbers in the test section while maintaining choked flow in the inlet with centerbody. The rpm of the compressor was reduced accordingly.

#### 4. RESULTS AND DISCUSSION

Figures 7 to 9 show the far-field attenuation of the three modes due to flow for two Mach number settings. In each case the generated frequency is slightly above the cut-on frequency for that mode even at the higher Mach number. Figure 10 shows that for a given duct, higher modes are cut on as a result of increasing the flow Mach number.

Figure 11 presents a comparison of sound attenuation due to flow for the four inlets tested. Since there are significant angular variations in the far-field noise levels, an average value is used in this comparison. Theoretical results from Reference 1 and experimental data both indicate that inlet configuration number three (constant velocity gradient) imparts the most momentum to the acoustic waves.

Figure 12 shows a typical noise attenuation pattern due to flow for a frequency that is high enough to cut on higher-order modes. Note that the noise level at first increases with increasing velocity; only when the flow approaches choke is a substantial noise reduction obtained. This large noise reduction is rarely achieved until the percentage of maximum mass flow is above 99. For inlets which are improperly designed aerodynamically, some noise reduction is obtained at low speeds, but at higher speeds large noise reductions are not observed as seen in Figure 13. This is consistent with results reported earlier in References 2 and 3. It should be noted that in the transonic compressor tests conducted in Reference 3, the noise level nearly always increased before decreasing at an average throat Mach number of above 0.9 (or 99 percent of maximum mass flow) as shown in Figure 14. In the case of an ejector, however, a plane wave exists; thus no increase in the noise level is observable with increasing Mach number. The

noise reduction is at first rather gradual with increasing flow velocity, but becomes abrupt near Mach one (for more details, refer to Reference 4).

## 5. CONCLUSION

A special facility has been successfully designed to study the influence of high-speed flow on noise of different frequencies and modes. It has been shown that high Mach number inlets can increase noise propagation rather than decrease it. This is due to the fact that the cutoff frequency is decreased by a factor of  $(1-M^2)^{1/2}$ , where  $M$  is the Mach number. The inlet with a constant axial gradient had the best performance acoustically and aerodynamically when compared to inlets with the same area ratio but with steep gradients near the throat or the exit. If high losses are encountered in the inlets, large noise reductions are not obtained even though the flow in the inlet is choked. More comprehensive results for the near as well as the far field are given in Reference 5.

Acknowledgement: Mr. Don Lansing, NASA Langley Research Center, has made helpful suggestions on inlet design. Mr. Tag, Mr. Cherng, and Mr. Kitayama of the University of Tennessee assisted in all phases of this research effort.

## REFERENCES

- 1 E. Lumsdaine and S. Ragab, "Effect of Flow on Plane Wave Propagation in a Variable-Area Duct of Finite Length," submitted for publication.
- 2 E. Lumsdaine, "Results of the Development of a Choked Inlet," Inter-Noise Proceedings, 1972, pp. 501-506.
- 3 E. Lumsdaine, J.G. Cherng, I. Tag, "Noise Suppression with High Mach Number Inlets," NASA CR-2708, June 1975.
- 4 E. Lumsdaine and L. Clark, "Noise Suppression with Sonic and Near-Sonic Inlets," Proceedings of the Second Interagency Symposium on University Research on Transportation Noise, North Carolina State University, 1974, pp. 432-447.
- 5 E. Lumsdaine, J.G. Cherng, I. Tag, "Influence of High-Speed Flow on Sound Propagation and Radiation," NASA Contractor Report, November 1976.



Fig. 1 Experimental setup to determine the influence of high-speed flow on noise attenuation.

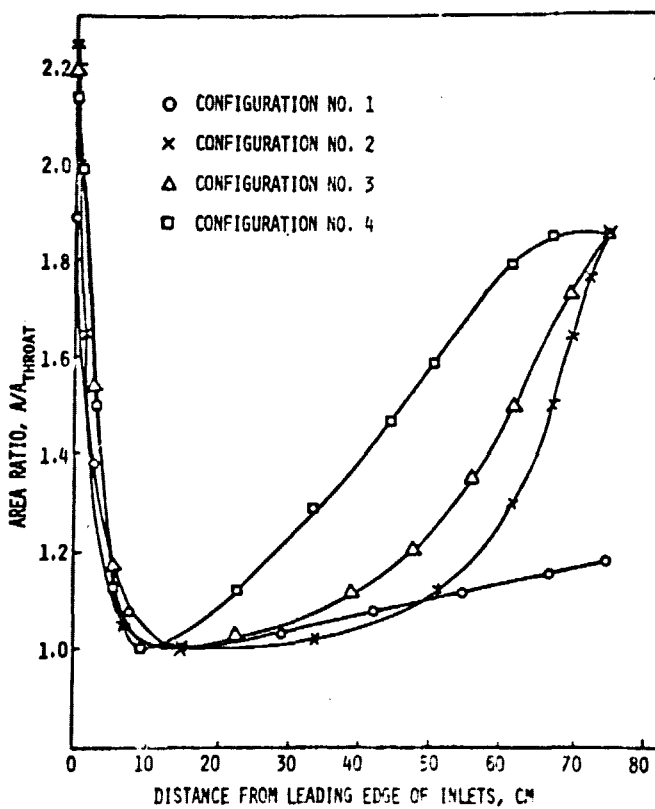


Fig. 2 Area distribution of inlet test sections.

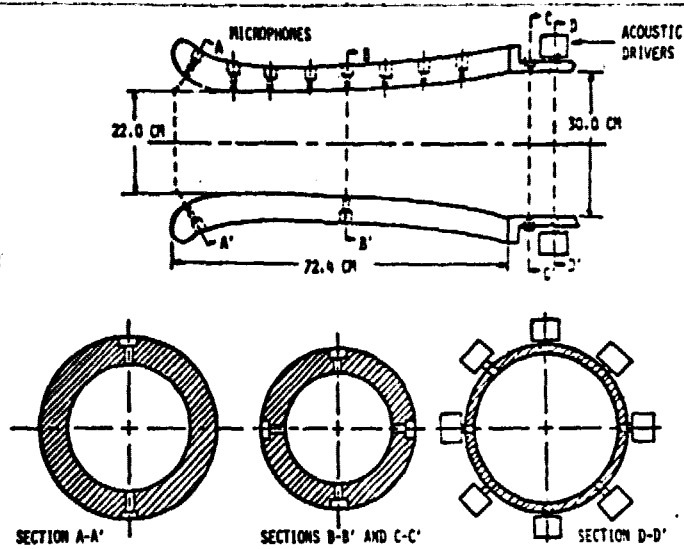


Fig. 3 Schematic of typical test section showing the microphone positions and location of acoustic drivers.

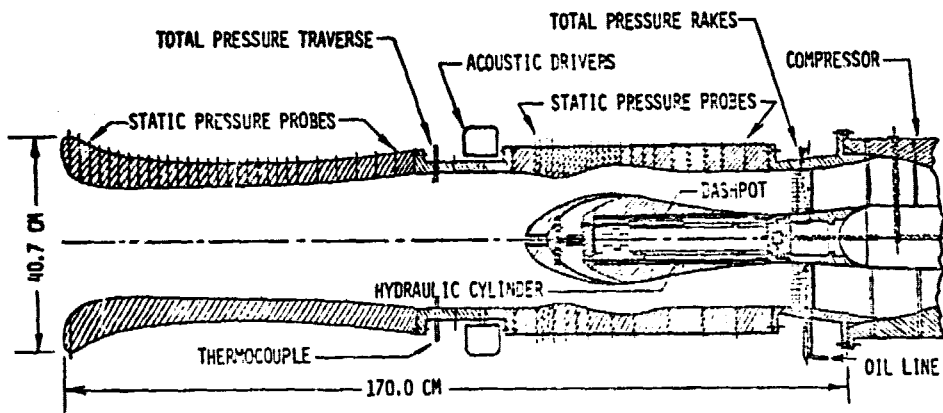


Fig. 4 Schematic of experimental apparatus showing test section and choked inlet with aerodynamic instrumentation.

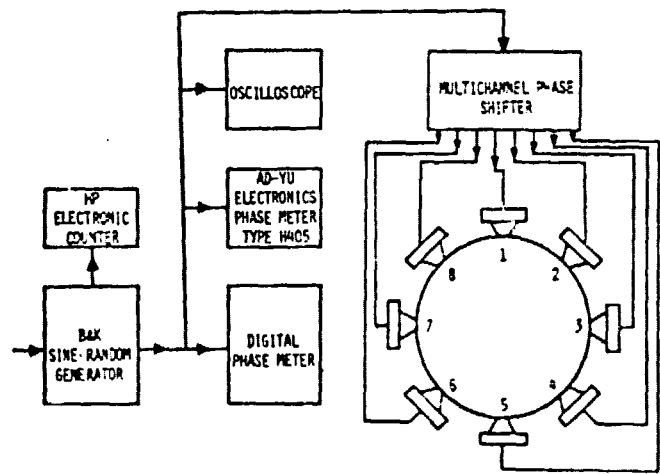
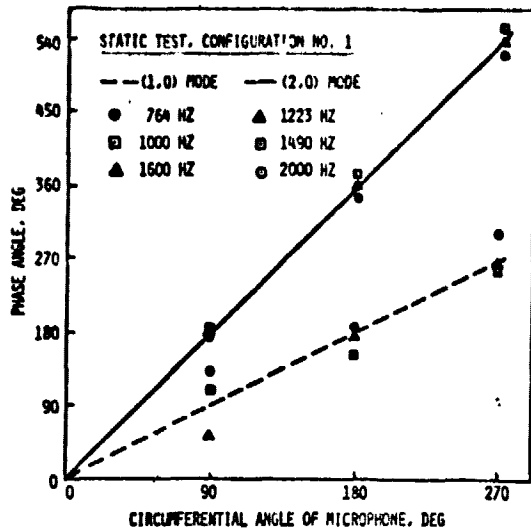


Fig. 5 Monitoring system for acoustic drivers.



DATA POINTS, FLUSH LEFT

DATA POINTS, LOWER CASE, FLUSH LEFT

Fig. 6 Variation of phase angle with microphone position.

Fig. 7 Far-field sound pressure level for inlet tested under flow conditions.

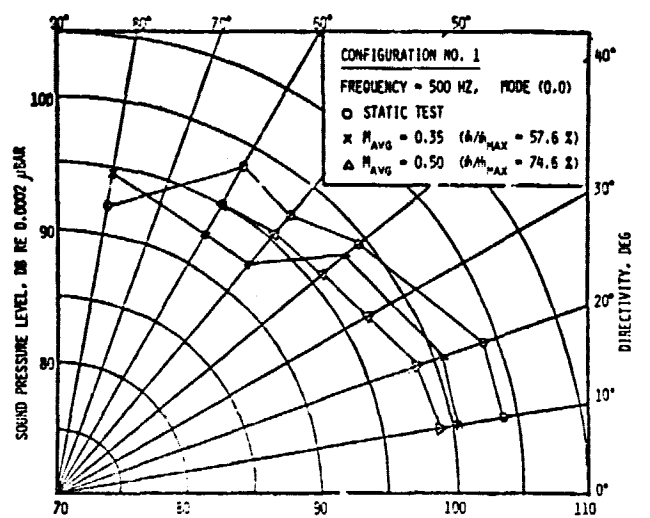


Fig. 8 Far-field sound pressure level for inlet tested under flow conditions.

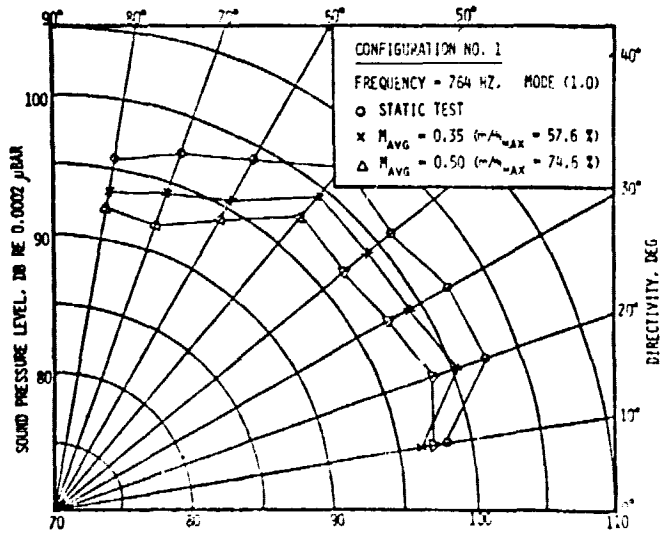




Fig. 9 Far-field sound pressure level for inlet tested under flow conditions.

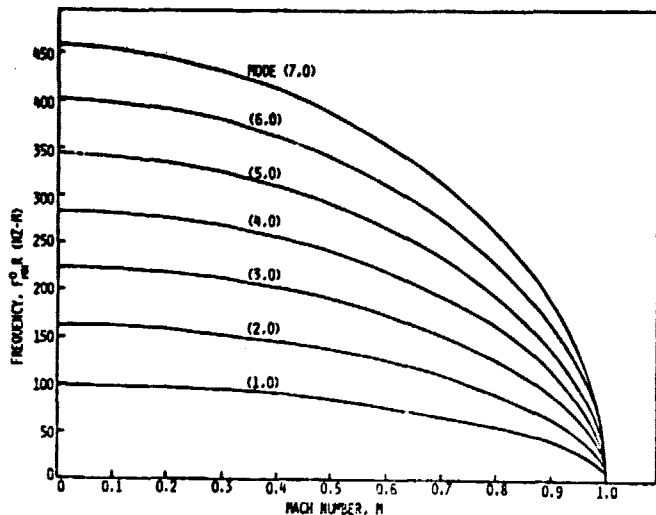
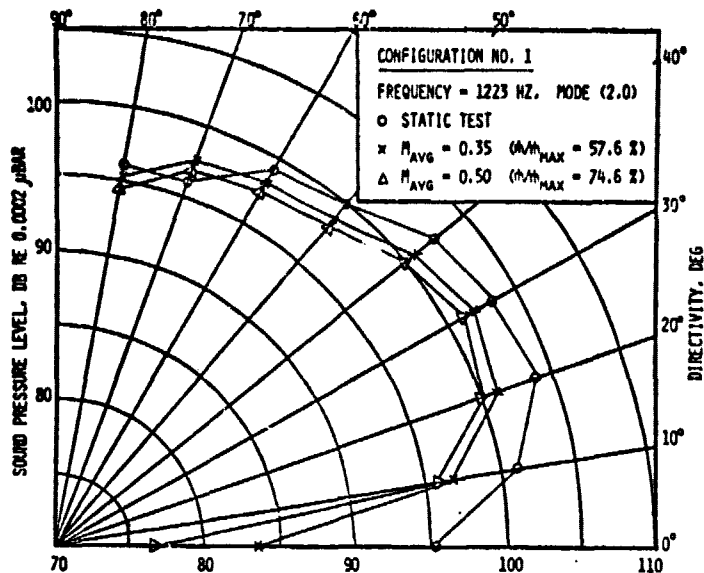


Fig. 10 Cut-off frequency as a function of Mach number for a constant-area duct.

Fig. 11 Comparison of sound attenuation due to flow for the four inlets tested.

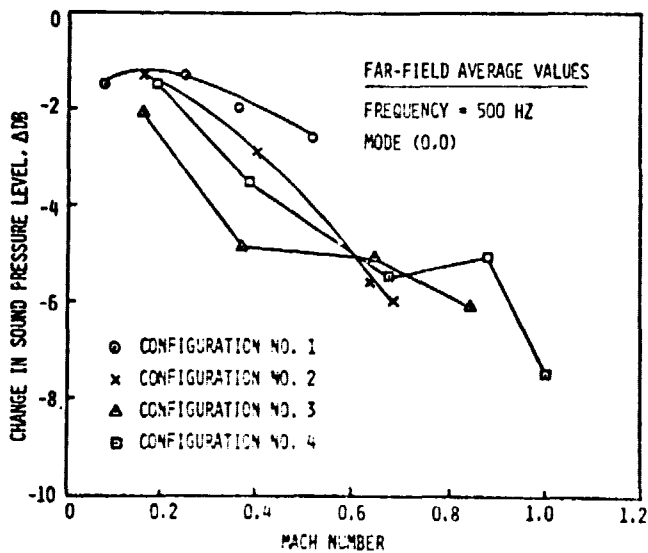


Fig. 12 Far-field sound pressure level for inlet configuration No. 3 under flow conditions.

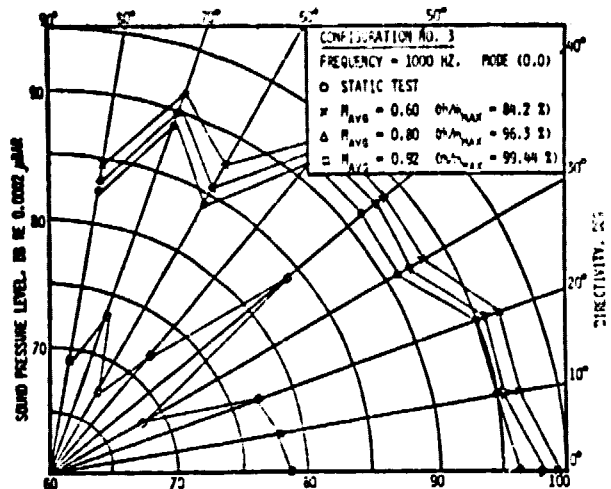


Fig. 13 Far-field sound pressure level for inlet configuration No. 4 under flow conditions.

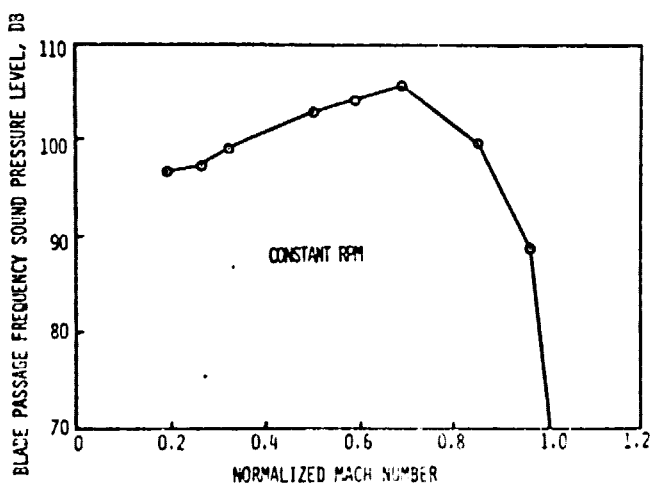
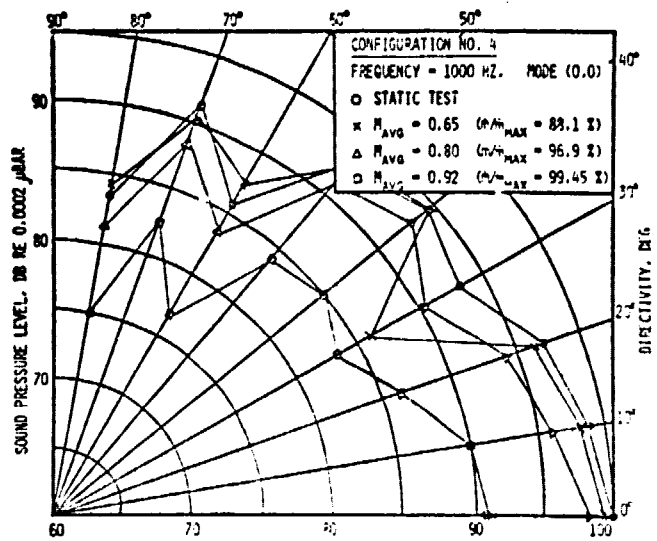


Fig. 14 Effect of flow on the blade passage frequency sound pressure level (compressor source).